This is an open access article published under a Creative Commons Non-Commercial No Derivative Works (CC-BY-NC-ND) Attribution License, which permits copying and redistribution of the article, and creation of adaptations, all for non-commercial purposes.

ACS AUTHORCHOICE

Macromolecules

pubs.acs.org/Macromolecules Article

Influence of Regioregularity on the Optoelectronic Properties of Conjugated Diketopyrrolopyrrole Polymers Comprising Asymmetric Monomers

Pieter J. Leenaers, Harm van Eersel, Junyu Li, Martijn M. Wienk, and René A. J. Janssen*

Cite This: *Macromolecules* 2020, 53, 7749–7758 Read Online

ACCESS | Metrics & More | Article Recommendations | Supporting Information

ABSTRACT: Two asymmetric thiophene (T)/pyridine (Py) flanked diketopyrrolopyrrole (DPP) polymers with a regiorandom and regioregular conjugated backbone are synthesized via a Stille polycondensation to investigate the effect of regioregularity on their optoelectronic properties and photovoltaic performance in fullerene-based polymer solar cells. Surprisingly, both polymers possess very similar optical bandgap, energy levels, and photovoltaic performance. These findings, combined with a factor of 19 reactivity difference between the two end groups of the asymmetric DPP monomer, intuitively suggest the formation of regular chain segments in the random polymer. However, by modeling the random polymerization reaction with a kinetic Monte Carlo (KMC) simulation, evidence is obtained for exclusive formation of a fully random polymer structure. UV–vis–NIR absorption spectra of three extended DPP chromophores, containing the donor segments (T-T-T, Py-T-Py, and Py-T-T) present in the regiorandom polymer, confirm that regioregularity of the backbone has a negligible influence on the optical properties.

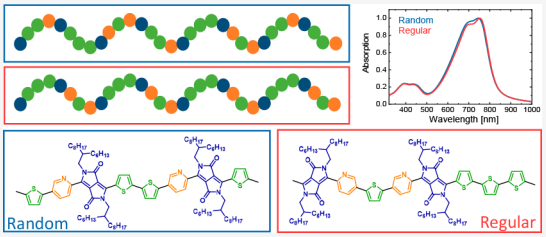

INTRODUCTION

Advancements in the design and synthesis of semiconducting conjugated polymers are the main contributor to the excellent performance of modern organic electronic devices.[1−6] A major breakthrough in the design of conjugated polymers was achieved by the D−A approach,[7] in which electron donating (D) and electron accepting (A) units are alternating along the conjugated polymer backbone to tune the optoelectronic properties such as orbital energy levels and optical bandgap.[8,9]

Coupled to the intrinsic optoelectronic properties of the polymer is its structural organization (or morphological order) in the solid state which is also important for device performance because it determines the bulk properties of the material such as charge carrier mobility.[10] Control over structural organization of conjugated polymers in the solid state can be challenging as it depends not only on intrinsic factors such as the nature of the solubilizing side chains,[11] the molecular weight distribution,[12−14] end-group contributions,[15] and the exact sequence and orientation of units in the conjugated polymer backbone[16,17] but also on extrinsic factors such as substrate type,[18] used solvent system,[14,19,20] and (thermal) annealing steps.[21−23]

A classic example of the effect of structural organization of a conjugated polymer in the solid state on the performance in organic electronic devices involves poly(3-hexylthiophene) (P3HT). Because of the asymmetric nature of the 3-hexylthiophene repeat unit, the exact structure of the conjugated polymer backbone depends on the relative orientation of the repeat units (head-to-head, tail-to-tail, or head-to-tail) and the amount of segments with different relative orientation in the chain, leading to polymers with different degrees of regioregularity. P3HT batches with a high degree of regioregularity have shown higher levels of crystallinity, red-shifted absorption spectra,[16] and higher charge carrier mobility[24] when compared to batches with a lower degree of backbone regularity. Furthermore, polymer solar cells made from P3HT with a high degree of regioregularity outperformed cells made from a batch with a low regioregularity.[16]

Next to P3HT, several conjugated polymers with asymmetric D or A units in their backbone have been designed over recent years. Also for these polymers, control over the exact orientation and sequence of the asymmetric units (regioregularity control) was demonstrated to be important in terms of hole mobility and solar cell performance.[25−35] However, a recent comparison between regiorandom and regioregular 5-fluoro-2,1,3-benzothiadiazole (FBT) polymers questions the superior design of regioregular polymers since the regiorandom polymer in these studies had a higher hole mobility[36,37] and significantly improved performance in polymer solar cells.[37] Another class of asymmetric D−A polymers for which

Received: July 18, 2020
Published: September 1, 2020

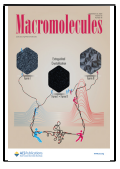

ACS Publications © 2020 American Chemical Society

https://dx.doi.org/10.1021/acs.macromol.0c01655
Macromolecules 2020, 53, 7749–7758

Scheme 1. Structure and Synthesis of the Regiorandom Polymer (P(TDPPPy-T)-*ran*) and the Regioregular Polymer (P(TDPPPy-T)-*reg*)[a]

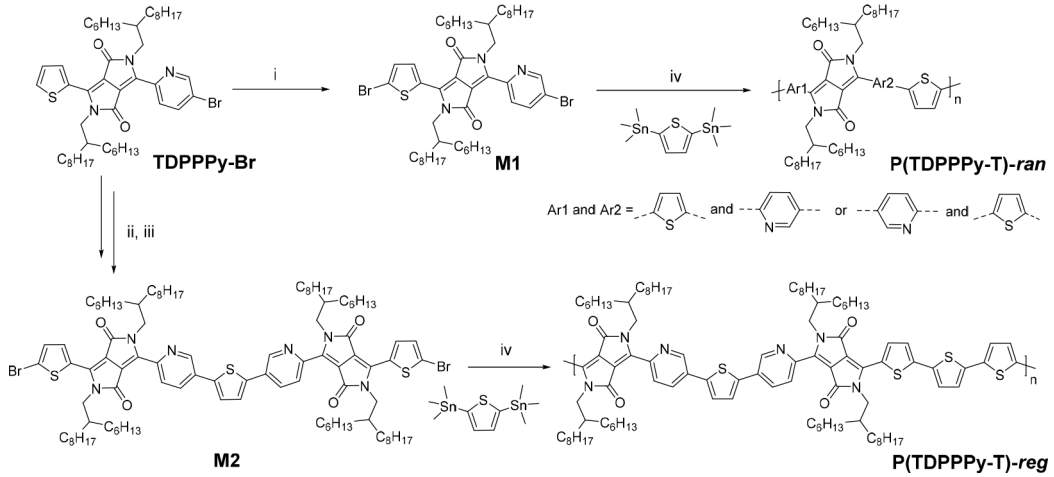

[a]Reagents and conditions: (i) NBS, $CHCl_3$, 0 °C; (ii) 2,5-bis(trimethylstannyl)thiophene, $Pd_2(dba)_3/PPh_3$, toluene/DMF (9:1, v/v), 115 °C; (iii) NBS, $CHCl_3$, 0 °C; (iv) $Pd_2(dba)_3/PPh_3$, toluene/DMF (9:1, v/v), 115 °C.

regioregularity control of the backbone is important are based on thieno[3,4-*b*]thiophene (TT). By synthesizing a regioregular PBDTTT-C-T polymer based on alternating benzo[1,2-*b*:4,5-*b*′]dithiophene (BDT) with perfectly controlled TT orientation, Lee et al.[38] showed that the regioregular polymer has a higher degree of crystallinity, a higher charge carrier mobility, and improved photovoltaic performance compared to the regiorandom isomer.

Despite various comparative studies between regioregular and regiorandom asymmetric conjugated polymers, a thorough understanding of the actual conjugated backbone structure of regiorandom asymmetric polymers is still lacking. By performing NMR spectroscopy on regiorandom polymers, some studies have confirmed the statistical distribution of different segments in the polymer chain.[27,36,37,39] However, studies that actually quantify the amount of different segments present in the chain are rare.[37] In 2014, Zhong and co-workers[25] investigated the effect of the regio- and chemoselectivity of an asymmetric fluoro-substituted thieno[3,4-*b*]thiophene (FTT) monomer during its conventional one-pot polymerization with BDT on the distribution of different segments in the polymer backbone. They found that due to the specific regio- and chemoselectivity of the FTT monomer, two distinct segments (A and B) were formed in the PTB7-Th polymer backbone in a 0.36/0.64 ratio. In segment A, the fluorine atoms on the FTT unit point in the same direction while in segment B the orientation of the fluorine atoms alternates. By comparison with the neat regioregular polymers consiting of only A or only B segements, they showed that in the random polymer segment B i leads to superior absorption, packing order, and charge mobility.[29]

In 2016, asymmetric DPP polymers with two different aromatic flanking units next to the DPP unit were synthesized by conventional one-pot Stille polymerization and implemented in organic field-effect transistors (OFETs) and polymer solar cells (PSCs) by Li et al.[40] Since then, many new asymmetric DPP polymers have been synthesized in an identical manner and been applied in OFET and/or PSC devices.[40−48] Besides examples of asymmetric DPP polymers with a presumed random polymer backbone[40−48] (due to one-pot polymerization), Saeki et al.[49] were the first to report a regioregular asymmetric DPP polymer, sandwiching a BDT unit between two thiophene (T)/pyridine (Py) flanked DPP units in a centrosymmetric fashion. The regioregular polymer displayed a higher hole mobility in pristine films than the regiorandom isomer (PPy), but its photovoltaic performance in fullerene-based solar cells was less. Comparison of the optical and electrochemical bandgap between the regular and random asymmetric DPP polymers of Saeki et al.[49] revealed an intriguing similarity, despite the differences in regioregularity of the conjugated polymer backbones.

In this contribution we synthesize a new regioregular asymmetric DPP polymer (**P(TDPPPy-T)-*reg***) composed of a thiophene (T)/pyridine (Py) flanked DPP acceptor unit and a thiophene donor unit and compare its optoelectronic properties and photovoltaic performance in PSCs with a presumed random asymmetric T/Py flanked DPP polymer (**P(TDPPPy-T)-*ran***). We find that next to their virtually identical absorption spectra and energy levels, the polymers have different hole mobilities but behave quite similar in photovoltaic devices. To address the similarities between both polymers and investigate the effect of regioselectivity of the asymmetric DPP monomer on the structure of **P(TDPPPy-T)-*ran***, kinetic Monte Carlo (KMC) simulations of the one-pot polymerization reaction are performed to determine the relative abundance of the three different possible donor segments (T-T-T, Py-T-Py, and Py-T-T) in the conjugated backbone of **P(TDPPPy-T)-*ran*** using reaction rate constants obtained from a model reaction. The KMC simulations show that the backbone of **P(TDPPPy-T)-*ran*** significantly differs from the backbone of **P(TDPPPy-T)-*reg*** and is truly random, despite an almost 20-fold regioselectivity of the two termini of the asymmetric T-DPP-Py monomer. The similarities in optoelectronic properties between both polymers are explained by averaging of the bandgap of the different donor segments within the conjugation length of the random polymer.

RESULTS AND DISCUSSION

Materials Synthesis and Characterization. The regiorandom (**P(TDPPPy-T)-*ran***) and regioregular (**P(TDPPPy-T)-*reg***) polymers were synthesized via Stille polymerization of

https://dx.doi.org/10.1021/acs.macromol.0c01655
Macromolecules 2020, 53, 7749−7758

Table 1. Physical Properties of the Polymers

polymer	M_n [kDa]	M_w [kDa]	$Đ$	$E_{g,opt}$[a] [eV]	HOMO[b] [eV]	LUMO[b] [eV]	$E_{g,swv}$[c] [eV]	ref
P(TDPPPy-T)-*ran*	46.6	122	2.6	1.49	−5.16	−3.20	1.96	this work
P(TDPPPy-T)-*reg*	93.3	249	2.7	1.49	−5.19	−3.20	1.99	this work
PDPP3T	147	400	2.7	1.33	−4.93	−3.13	1.80	52
PDPP2PyT	67.4	176	2.6	1.73	−5.41	−3.19	2.22	53

[a]From the absorption onset in thin films. [b]From square-wave voltammetry using −4.59 eV[54] for the energy of Fc/Fc^+. [c]Electrochemical bandgap.

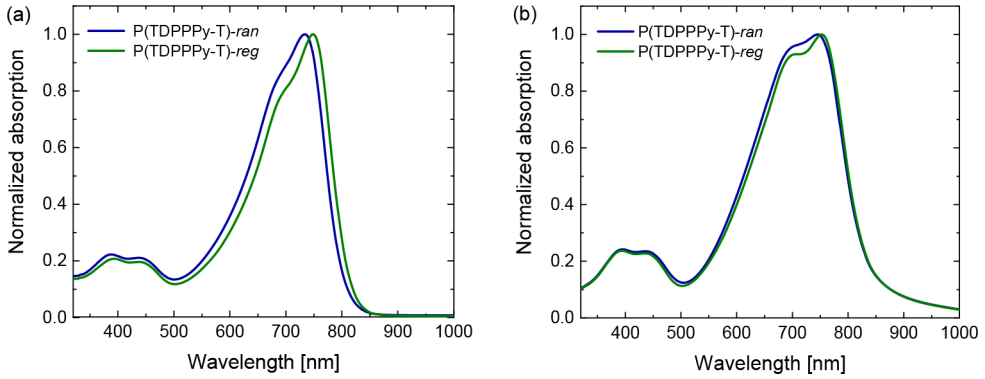

Figure 1. Normalized UV−vis−NIR absorption spectra of the regiorandom (**P(TDPPPy-T)**-*ran*) and regioregular (**P(TDPPPy-T)**-*reg*) asymmetric DPP polymers: (a) in chloroform solution; (b) as thin film on glass.

2,5-bis(trimethylstannyl)thiophene (**Sn-T-Sn**) with the asymmetric (**M1**) and centrosymmetric (**M2**) dibrominated DPP monomers, respectively (Scheme 1). **M1** was synthesized according to modified literature procedures.[44,50] **M2** was synthesized by a Stille type coupling reaction between the monobrominated **TDPPPy-Br** precursor and **Sn-T-Sn** and subsequent bromination with *N*-bromosuccinimide (NBS). A detailed description of the monomer synthesis and structural characterization of the intermediates can be found in the Supporting Information.

As shown in Scheme 1, the exact structure of the **P(TDPPPy-T)**-*ran* conjugated backbone is ill-defined due to formation of different donor blocks (T-T-T, Py-T-Py, and Py-T-T) during the conventional one-pot polycondensation reaction. Therefore, as for all asymmetric DPP polymers in the literature,[40−48] it is assumed that the distribution of the different donor blocks in the conjugated backbone of **P(TDPPPy-T)**-*ran* is random. Use of the centrosymmetric DPP monomer (**M2**) ensures the formation of a regioregular polymer (**P(TDPPPy-T)**-*reg*) with a defined alternating structure of Py-T-Py and T-T-T blocks.

Both polymerizations were performed under optimized reaction conditions,[51] and after purification by Soxhlet extraction with acetone, *n*-hexane, and dichloromethane (DCM), the polymers were obtained by precipitation in methanol. The molecular weights and polydispersity of both polymers are given in Table 1 and were determined by gel permeation chromatography (GPC) in *o*-DCB at 140 °C to reduce the effect of aggregation on the molecular weight analysis. The number-average molecular weight (M_n) of **P(TDPPPy-T)**-*reg* is 2 times higher than the M_n of **P(TDPPPy-T)**-*ran*. However, since both polymers still showed signs of aggregation in the inline UV−vis−NIR spectra taken during elution from the size-exclusion column, their molecular weights are possibly overestimated.

Obtaining symmetric DPP polymers from the DCM fraction, instead of the chloroform or 1,1,2,2-tetrachloroethane (TCE) fraction, in the Soxhlet extraction procedure usually indicates formation of highly soluble polymers and/or polymers with a low molecular weight. Because the molecular weights of both asymmetric DPP polymers are above 40 kDa, both must have a relatively high solubility compared to their symmetric derivatives, PDPP3T[51] and PDPP2PyT.[52] Indeed, both polymers show good solubility in common organic solvents such as DCM, chloroform, chlorobenzene, and even toluene. Considering the high molecular weight and regularity of **P(TDPPPy-T)**-*reg*, the asymmetry in the conjugated backbone of the polymer must be responsible for its good solubility in nonhalogenated solvents as observed before by Li et al.[40] for other asymmetric DPP polymers.

Optical and Electrochemical Properties. The optical properties of the regiorandom and regioregular polymers were investigated by UV−vis−NIR absorption spectroscopy in chloroform solution and in thin film (Figure 1). Two characteristic bands can be observed in both solution and thin film spectra. The weak band around 400 nm originates from localized $\pi-\pi^*$ transitions, while the intense band at 700 nm is related to intramolecular charge transfer (ICT) between the different donor blocks (T-T-T, Py-T-Py, and Py-T-T) and the DPP acceptor unit. The absorption spectrum of the regioregular polymer in solution shows a bathochromic shift (10 nm) and a slightly different intensity ratio between the 0−0 and 0−1 vibronic peaks in comparison with the solution spectrum of the regiorandom polymer. The vibrational splitting is characteristic for aggregated DPP polymers.[55] Comparison of the temperature-dependent absorption spectra of both polymers (Figure S1, Supporting Information) in TCE shows that the regioregular polymer retains this higher ratio between the 0−0 and 0−1 vibronic peaks at elevated temperatures. This indicates that the regioregular polymer has a higher degree of aggregation than the regiorandom polymer. It also demonstrates that despite their higher solubility compared to symmetric polymers, these asymmetric substituted DPP polymers are not fully molecularly dissolved.

When going from solution to solid state, both absorption spectra broaden and exhibit a red-shift of about 20 nm which

https://dx.doi.org/10.1021/acs.macromol.0c01655
Macromolecules 2020, 53, 7749−7758

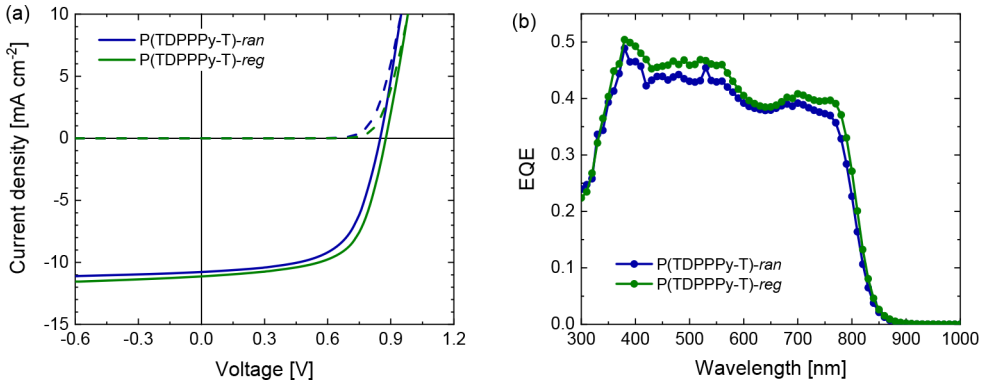

Figure 2. (a) $J-V$ characteristics (under simulated AM1.5G illumination) of optimized polymer:[70]PCBM (1:2 w/w) solar cells based on the regiorandom (**P(TDPPPy-T)**-*ran*) and regioregular (**P(TDPPPy-T)**-*reg*) asymmetric DPP polymers. (b) Corresponding EQE spectra.

can be attributed to intermolecular $\pi-\pi$ interactions. Both polymers have similar spectral shapes in thin film with identical optical bandgaps of 1.49 eV (834 nm), determined from the onset of absorption. The bandgap of both polymers in thin film lies close to the mathematical average (1.53 eV) of their symmetric counterparts, PDPP3T[51] and PDPP2PyT,[52] for which optical bandgap data are shown in Table 1. The small difference in intensity ratio between the 0−0 and 0−1 peaks in solution and thin film can probably be related to the higher molecular weight of the regioregular polymer, which causes the higher degree of aggregation.

The frontier molecular orbital energy levels (HOMO and LUMO) of both polymers were estimated by square-wave voltammetry from the first onset of the oxidation (E_{ox}) and reduction potential (E_{red}) (Figure S2), on thin films on a platinum wire working electrode. The energy levels are presented in Table 1. The HOMO levels of the regiorandom and regioregular polymer are situated between the HOMO levels of PDPP3T and PDPP2PyT. The LUMO levels of both polymers are equal and lie close to the LUMO of PDPP2PyT. The observed similarity in LUMO levels could originate from spatial localization around the thiophene/pyridine flanked DPP acceptor unit. The HOMO of the regiorandom polymer is 30 meV higher than the HOMO of the regioregular polymer, likely due to the presence of Py-T-T donor blocks.

Photovoltaic Properties and Charge Carrier Mobilities. The impact of regioregularity on the photovoltaic performance was investigated by fabrication of PSCs with the polymers as electron donor and [6,6]-phenyl-C_{71}-butylric acid methyl ester ([70]PCBM) as electron acceptor in a conventional device architecture (ITO/MoO_3/polymer:[70]PCBM/LiF/Al). Solar cells of the regiorandom polymer fabricated on a conventional PEDOT:PSS hole extraction layer showed S-shaped $J-V$ characteristics (Figure S3). To prevent this behavior, also previously observed for devices with active layers containing aromatic amines deposited on PEDOT:PSS,[52,56] a 10 nm evaporated MoO_3 layer was used instead.

Devices of both polymers fabricated from chloroform containing 2% 1,8-diiodooctane (DIO) as cosolvent showed a substantial bias-dependent photocurrent with a low fill factor (FF) around 0.40, when the cast layers were dried in ambient air. When the cast layers were directly transferred to a vacuum after spin coating, the bias dependency of the photocurrent disappeared (Figure S3), resulting in improved FFs (Tables S1 and S2). Likely, the morphology of the active layer is unfavorably affected by the slow drying cosolvent, while quick drying in vacuum ($\approx 10^{-2}$ mbar) results in a more optimal morphology which removes the bias dependency of the photocurrent and improves the FF.

The photovoltaic performance for each polymer was optimized for layer thickness and for type and amount of cosolvent (Tables S1 and S2). Chloroform was used as the main solvent, and the polymers were combined with [70]PCBM in a 1:2 weight ratio, respectively.[57] For both polymers 5 vol % diphenyl ether (DPE) was found to be the optimal amount of cosolvent.

Current density−voltage ($J-V$) characteristics and external quantum efficiency (EQE) of the optimized solar cells based on the regiorandom and regioregular polymer are shown in Figure 2, and the characteristic device parameters are summarized in Table 2. Surprisingly, **P(TDPPPy-T)**-*reg* only slightly outperforms **P(TDPPPy-T)**-*ran* with power conversion efficiencies (PCEs) of 6.6% vs 5.9% due to minor improvements in short-circuit current density (J_{sc}), open-circuit voltage (V_{oc}), and FF. The 30 mV lower V_{oc} of **P(TDPPPy-T)**-*ran* compared with **P(TDPPPy-T)**-*reg* matches with its higher HOMO energy level. The J_{sc} of the regioregular polymer is only 0.7 mA cm^{-2} higher than the J_{sc} of the regiorandom polymer, which is corroborated by the enhanced external quantum efficiency (EQE) over the entire spectral range.

Table 2. Device Characteristics of PSCs Based on Blends of P(TDPPPy-T)-*ran* and P(TDPPPy-T)-*reg* with [70]PCBM[a]

polymer	d [nm]	J_{sc} [mA cm^{-2}]	V_{oc} [V]	FF	PCE [%]
P(TDPPPy-T)-*ran*	108	11.2	0.85	0.61	5.9
P(TDPPPy-T)-*reg*	96	11.9	0.88	0.63	6.6

[a]Best performing devices are shown. Average characteristics can be found in Table S3.

Charge carrier mobilities of the two polymers in the blends with [70]PCBM were estimated by analyzing the space-charge-limited current in hole-only devices (Figure S4). The current density was fitted to the Murgatroyd relation $J = (9/8)\varepsilon_0\varepsilon_r\mu_0(V^2/L^3)\exp[0.89\gamma(V/L)^{1/2}]$ for space-charge-limited current with field-dependent mobility,[58,59] with ε_0 the vacuum permittivity, ε_r the relative permittivity of the polymers (approximated to be 3.5), μ_0 the zero-field mobility, L the thickness of the organic layer, and γ the field-activation factor. The voltage was corrected for built-in potential and series resistance. The hole mobility is about 3.3×10^{-6} cm^2 V^{-1} s^{-1}

https://dx.doi.org/10.1021/acs.macromol.0c01655
Macromolecules 2020, 53, 7749−7758

for **P(TDPPPy-T)**-*ran*) and 8.4×10^{-4} cm^2 V^{-1} s^{-1} for **P(TDPPPy-T)**-*reg*.

Morphology of the Blends. Transmission electron microscopy (TEM) was performed on the optimized active layers of PSCs based on the regiorandom and regioregular polymer to investigate the origin of their difference in EQE (and thus also J_{sc}). Both asymmetric DPP polymers exhibit the characteristic fibrous-like morphology known for symmetric DPP polymers when blended with PCBM (Figure 3). The morphology of the photoactive layer with the regioregular polymer (Figure 3b) appears to have slightly narrower fibers than the morphology of the regiorandom polymer based layer (Figure 3a), which is consistent with the small difference in EQE and J_{sc}.

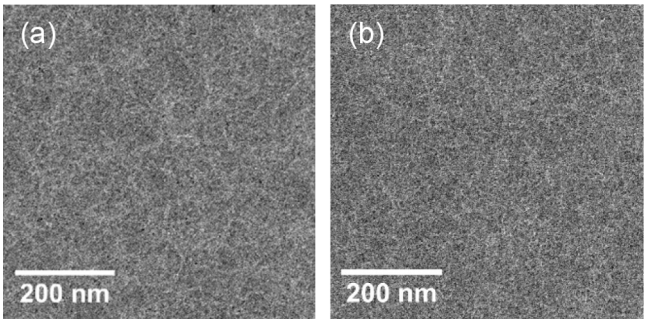

Figure 3. TEM images of the optimized photoactive layers based on (a) the regiorandom (**P(TDPPPy-T)**-*ran*) polymer and (b) the regioregular (**P(TDPPPy-T)**-*reg*) polymer.

Grazing incidence wide-angle X-ray scattering experiments were performed to investigate the influence of regioregularity of the asymmetric DPP polymers on molecular packing and crystallinity in the pristine polymer films and in their respective photovoltaic blends with [70]PCBM. The 2D GIWAXS patterns are shown in Figure S5, and the in-plane and out-of-plane line cuts extracted from the 2D data are shown in Figure 4. For the pristine polymer films, very broad (010) scattering peaks are observed around $q \approx 1.5$ $Å^{-1}$ corresponding to $\pi-\pi$ stacking of the conjugated polymer backbones. The intensity of the (010) peak for the regioregular polymer is significantly higher than for the regiorandom polymer (Figure 4, upper panels), which suggests that the regioregular polymer forms a higher amount of and/or more ordered $\pi-\pi$ stacked aggregates than the random polymer. There is little evidence for preferential orientation of the aggregates, as shown by the 2D patterns in Figure S5. For the blends with [70]PCBM, a scattering peak at $q = 1.34$ $Å^{-1}$ appears attributed to [70]PCBM aggregates. In the blends, the (010) peak of the regiorandom polymer is hardly visible, while the (010) peak of the regioregular polymer and the $q = 1.34$ $Å^{-1}$ peak of [70]PCBM coalesce into one broad diffraction peak. The absence of clear (h00) peaks for the pristine random and regular asymmetric DPP polymers and their blends with [70]PCBM indicates that the $\pi-\pi$ stacked aggregates do not assemble into long-range ordered lamellar crystallites.

Regioselectivity of the Stille Coupling. The strong similarity in optical absorption spectra, energy levels, and PSCs between the regiorandom and regioregular asymmetric DPP polymers questions the exact structure of the regiorandom polymer. If a high amount of T-T-T segments alternating with Py-T-Py blocks would be formed in the conventional one-pot polymerization reaction between **M1** and **Sn-T-Sn**, the small differences in optoelectronic properties and photovoltaic performance between both polymers would easily be explained.

A recent example of a random polymer with a substantial amount of a specific regioregular block in its conjugated backbone is PTB7-Th.[25] The regioregular block has a strong effect on the optoelectronic properties and photovoltaic behavior of the polymer, causing the random polymer to display similar optoelectronic properties and photovoltaic behavior under optimized conditions as a deliberately synthesized regioregular PTB7-Th polymer.[29] Formation of substantial amounts of the regioregular block in the backbone of the random polymer was assumed to occur during the initial stage of the one-pot polymerization, driven by the preferential regio- and chemoselectivity of the asymmetric FTT monomer and its A-D-A intermediate, respectively.[25] If the **M1** monomer would have a strong regioselectivity for reaction of **Sn-T-Sn** with the bromine on either the thiophene (T) or pyridine (Py) groups, A-D-A intermediates (Py-DPP-T-T-T-DPP-Py or T-DPP-Py-T-Py-DPP-T) might be formed preferentially, resulting in the formation of regioregular blocks upon further polymerization with the remaining **Sn-T-Sn**.

To investigate whether the asymmetric thiophene/pyridine DPP monomer (**M1**) has a certain regioselectivity for reaction

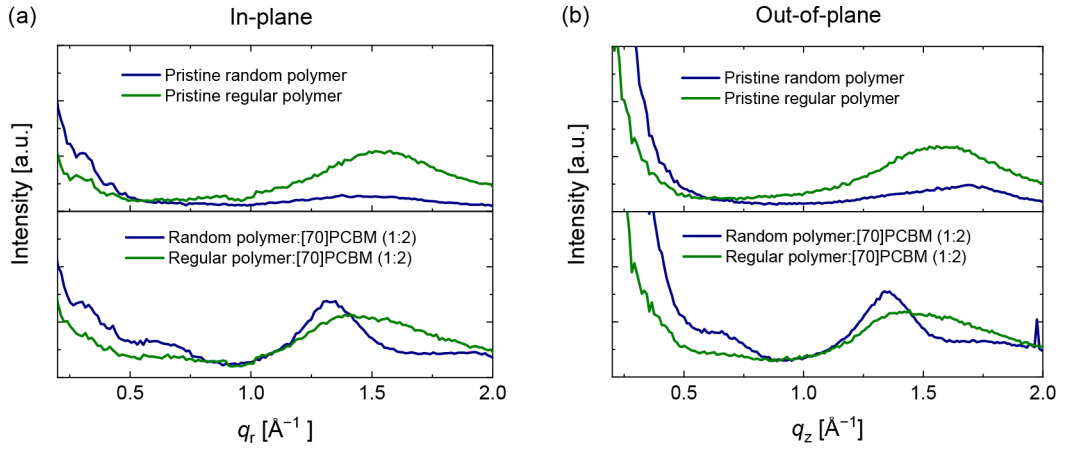

Figure 4. (a) In-plane and (b) out-of-plane 1D GIWAXS profiles of the regiorandom (blue) and the regioregular (green) polymer and their respective photovoltaic blends.

https://dx.doi.org/10.1021/acs.macromol.0c01655
Macromolecules 2020, 53, 7749−7758

Scheme 2. Model Reaction between M1 and Sn-T to Determine the Regioselectivity of M1[a]

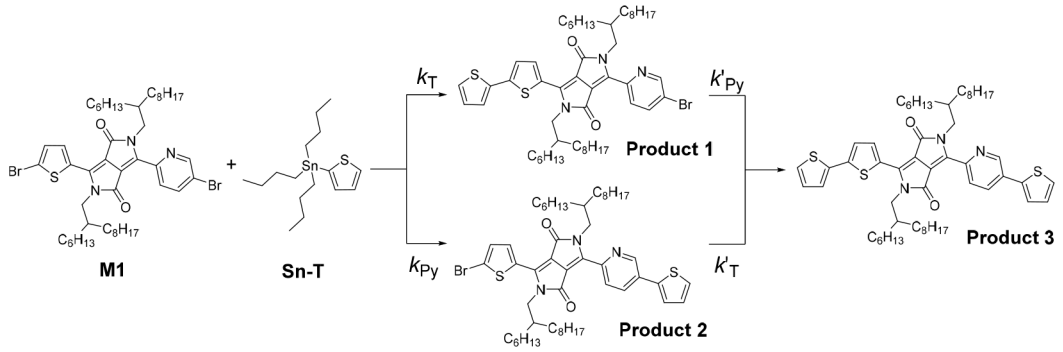

[a]It is assumed that $k_T = k'_T$ and $k_{Py} = k'_{Py}$.

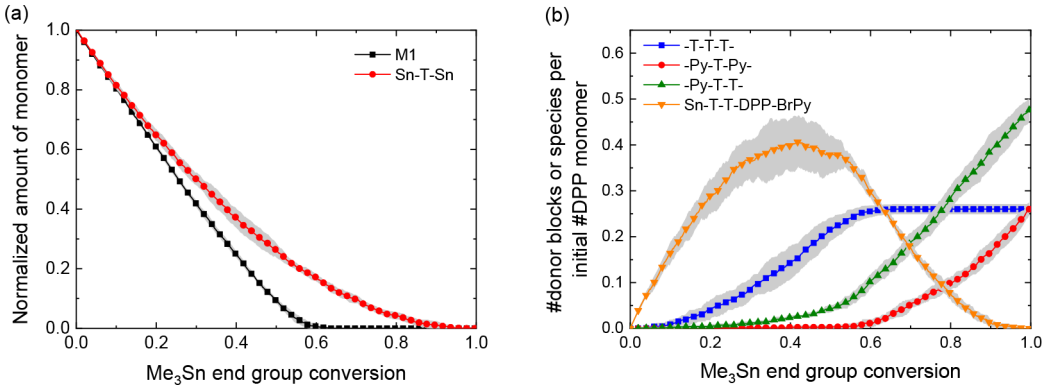

Figure 5. (a) Normalized amounts of **M1** and **Sn-T-Sn** monomers as a function of the Me_3Sn end-group conversion during KMC simulation of the one-pot polymerization reaction. (b) Fraction of donor blocks formed in the polymer per DPP unit present in the reaction as a function of the Me_3Sn end-group conversion during KMC simulation of the one-pot polymerization reaction. The gray areas show the error bars representing the standard deviation based on five simulations. Note: $k_T = 2.96 \times 10^{-3}$ s^{-1} and $k_{Py} = 1.56 \times 10^{-4}$ s^{-1}.

of **Sn-T-Sn** with one of its bromines, a model reaction between **M1** and a monostannylated thiophene (**Sn-T**) was performed (Scheme 2). Analysis by ^{1}H NMR spectroscopy (Figures S6 and S7) revealed a substantial amount of product **1** (90%) in the final (after 9000 s) reaction mixture of the model reaction, indicating a large regioselectivity for reaction of **Sn-T** with the Br-T terminus of **M1**. The reactivity difference between the thiophene and pyridine side of the asymmetric DPP monomer **M1** toward **Sn-T** was determined more accurately by fitting the product distributions obtained from the model reaction (Table S4) to the product distributions obtained from a differential rate equation model (Figure S8 and Table S5) for different rate constants (k_T and k_{Py}) (Scheme 2). The obtained rate constants were $k_T = 2.96 \times 10^{-3}$ s^{-1} and $k_{Py} = 1.56 \times 10^{-4}$ s^{-1}, resulting in a factor of 19 reactivity difference between the thiophene and pyridine side of the asymmetric **M1** monomer.

Kinetic Monte Carlo Simulation of the Polymer Backbone. To study whether the observed reactivity difference between the thiophene and pyridine side of **M1** can lead to a high amount of the regioregular—T-T-T alternating with Py-T-Py—block in the structure of **P(TDPPPy-T)**-*ran*, the one-pot polymerization between **M1** and **Sn-T-Sn** was modeled by using a KMC simulation with the determined rate constants as input parameters. In these simulations, it is assumed that k_T and k_{Py} do not depend on the length of the formed intermediate species. The simulation results (Figure 5) are plotted as a function of the trimethylstannyl (Me_3Sn) end-group conversion because this results in the typical asymptotic relation between the modeled average molecular weight and Me_3Sn end-group conversion (Figure S9), as experimentally observed for polycondensation reactions. Only at high Me_3Sn end-group conversion (>95%) are polymers with an applicable (>20 kDa) molecular weight formed.

Counting the different donor blocks (T-T-T, Py-T-Py, and Py-T-T) in the conjugated backbone of **P(TDPPPy-T)**-*ran* formed during the modeled random polymerization (Figure 5b) with experimental difference in rate constants of a factor of 19 between k_T and k_{Py} shows that the final amounts (at >95% Me_3Sn end-group conversion) of T-T-T and Py-T-Py blocks lie around 25%. This number is substantially lower than the amount of Py-T-T blocks (50%) which excludes the formation of a semiregioregular polymer, consisting of alternating T-T-T and Py-T-Py blocks with a small amount of Py-T-T defects. Even by simulating using a factors of 1 or of 1000 for the difference in rate constants between the two sides of the asymmetric DPP monomer (Figures S10 and S11), we find that the amount of formed Py-T-T blocks in the final polymer stays close to 50%, indicating that the regioselectivity of the asymmetric DPP monomer does not affect the randomness in the conjugated backbone of **P(TDPPPy-T)**-*ran*. This result is consistent with the combinatorial estimates made by Zhou et al.,[37] who determined that the amount of bithiophene segment in a random asymmetric FBT polymer must always be equal to or higher than 50%, similar to what we observe for the Py-T-T block.

https://dx.doi.org/10.1021/acs.macromol.0c01655
Macromolecules 2020, 53, 7749−7758

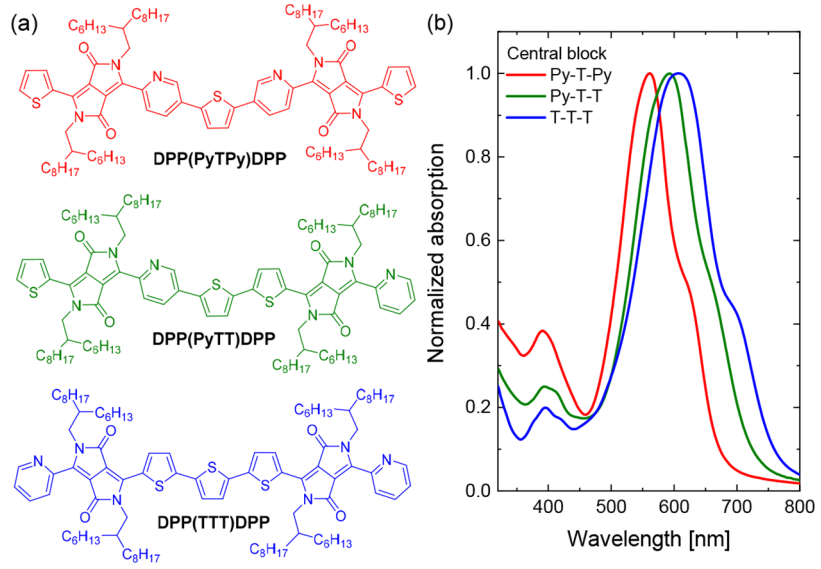

Figure 6. (a) Chemical structures of the extended isomeric DPP molecules containing the Py-T-Py, Py-T-T, and T-T-T central blocks found in the conjugated backbone of **P(TDPPPy-T)**-*ran*. (b) Corresponding optical absorption spectra.

The reason a (semi)regioregular DPP polymer cannot be obtained from the one-pot polymerization of the asymmetric DPP monomer can be seen in Figures 5a and 5b. At the start (0−15% conversion) of the one-pot polymerization, both monomers react away with the same rate (Figure 5a), but because of the faster reaction rate on the thiophene than on the pyridine side of the asymmetric monomer, the main reaction product is initially Sn-T-TDPP-Py-Br (Figure 5b). This intermediate product continues to be formed but is also used to make the T-T-T segments (Figure 5b), slowing down the incorporation rate of the **Sn-T-Sn** monomer (15−60% conversion). At some point (≈60% conversion), **M1** is depleted since it was rapidly build into the Sn-T-TDPP-Py-Br intermediate and T-T-T segments, leaving a constant amount of T-T-T segments in the reaction. At higher conversions, the formed oligomers start to form polymers by reacting with each other and with the residual amount of **Sn-T-Sn** monomer. But because the bromines on the pyridine side of the oligomers have almost been left untouched and there is still a substantial amount of Sn-T-TDPP-Py-Br left, Py-T-T blocks are formed in substantial amounts.

Models for Chain Segments. Having established that the random polymer is devoid of extended regioregular chain segments, we need to find an explanation for the similarity between the optical absorption spectra of **P(TDPPPy-T)**-*ran* and **P(TDPPPy-T)**-*reg*. The first point to note is that **P(TDPPPy-T)**-*reg* is a regioregular terpolymer built from three distinct π-conjugated units (DPP, T-T-T, and Py-T-Py). When compared to the corresponding copolymers PDPP3T and PDPP2PyT, each with only two π-conjugated units (DPP and T-T-T or DPP and Py-T-Py), one notices that the optical bandgap of **P(TDPPPy-T)**-*reg* (1.49 eV) is close to the arithmetic mean (1.53 eV) of the optical bandgaps of the PDPP3T (1.33 eV) and PDPP2PyT (1.73 eV). Apparently, the T-T-T and Py-T-Py segments form an "alloy" in the terpolymer. To check the properties of a Py-T-T segment as present in **P(TDPPPy-T)**-*ran*, we synthesized three extended isomeric DPP oligomers (Figure 6a), containing T-T-T, Py-T-Py, or Py-T-T blocks as central units. Their optical absorption spectra are shown in Figure 6b and reveal that the optical bandgap of the Py-T-T isomer (1.71 eV) is also close to the arithmetic mean (1.73 eV) of the optical bandgaps of the T-T-T (1.62 eV) and Py-T-Py isomers (1.84 eV). Both results indicate that the bandgap of the **P(TDPPPy-T)**-*ran* polymer is determined by averaging of the bandgap of the multiple different chromophore constituents within the effective conjugation length of its polymer backbone, resulting in an identical bandgap as the regioregular **P(TDPPPy-T)**-*reg* polymer.

CONCLUSION

We have synthesized a regioregular asymmetric DPP polymer (**P(TDPPPy-T)**-*reg*) composed of alternating T-T-T and Py-T-Py donor units. Alternation of T-T-T and Py-T-Py donor units in the conjugated backbone of **P(TDPPPy-T)**-*reg* is ensured by copolymerization of 2,5-bis(trimethylstannyl)-thiophene with a centrosymmetric DPP monomer (**M2**). We compared the optoelectronic properties of **P(TDPPPy-T)**-*reg* and its photovoltaic performance in fullerene-based PSCs with the corresponding regiorandom isomer (**P(TDPPPy-T)**-*ran*) made by conventional one-pot polymerization between 2,5-bis(trimethylstannyl)thiophene and an asymmetric thiophene/pyridine flanked DPP monomer (**M1**). **P(TDPPPy-T)**-*reg* and **P(TDPPPy-T)**-*ran* show nearly identical absorption spectra, energy levels, and optical bandgap, both in solution and in the solid state. Also, the photovoltaic performance of **P(TDPPPy-T)**-*reg* (PCE = 6.6%) in an optimized blend with [70]PCBM is very similar to that of **P(TDPPPy-T)**-*ran* (PCE = 5.9%).

Kinetic Monte Carlo simulations have been used to evaluate possible similarities between the intrachain structure of both isomers that might occur because of the very large (19-fold) difference in reactivity of the brominated pyridine and thiophene groups of the asymmetric DPP monomer **M1** in the Stille reaction. The KMC simulations show, however, that the similarities in optoelectronic properties and photovoltaic performance between both polymers are not due to similarities in the structure of their conjugated backbones. In the random polymer about 50% of the repeat units contain the asymmetric Py-T-T segment that does not occur in the **P(TDPPPy-T)**-*reg* polymer. Simulations of higher differences in reaction rate

https://dx.doi.org/10.1021/acs.macromol.0c01655
Macromolecules 2020, 53, 7749−7758

constants between the two sides of the asymmetric DPP monomer prove that a random structure, containing about 50% of Py-T-T blocks, is always being formed during its one-pot polymerization.

The similarity between the optoelectronic and device properties of **P(TDPPPy-T)**-*reg* and **P(TDPPPy-T)**-*ran* are thus the result of an alloying effect in which the effective conjugation along the chain causes the averaging of the energy levels with little sensitivity to the actual chain sequence. This conclusion is supported by the fact that the optical bandgap of the **P(TDPPPy-T)**-*reg* terpolymer is similar to the arithmetic mean of the optical bandgaps of PDPP3T and PDPP2PyT and by the optical absorption spectra of the three possible isomeric chromophore segments present in the conjugated chain of **P(TDPPPy-T)**-*ran* for which that of the Py-T-T segment is in between those of T-T-T and Py-T-Py.

These results demonstrate that conjugated polymers with a truly regiorandom backbone are inevitably formed during one-pot polymerizations of asymmetric monomers, independent of their regioselectivity. Randomness in the conjugated backbone of asymmetric DPP polymers, even when consisting out of distinctly different donor blocks, seems to have a negligible effect on optoelectronic properties and photovoltaic performance compared to a regioregular DPP terpolymer. Hence, avoiding the effort of synthesizing of extended symmetric DPP monomers does not deteriorate functional properties, which makes exploring random polymers from asymmetric monomers a useful strategy for exploring new conjugated materials.

■ ASSOCIATED CONTENT

Supporting Information

The Supporting Information is available free of charge at https://pubs.acs.org/doi/10.1021/acs.macromol.0c01655.

Detailed description of the monomer and DPP chromophore synthesis, molecular structural characterization, square-wave voltammetry, solar cell optimization, regioselectivity model reaction, graphs of the kinetic Monte Carlo simulation for different rate constant values (PDF)

■ AUTHOR INFORMATION

Corresponding Author

René A. J. Janssen − *Molecular Materials and Nanosystems & Institute for Complex Molecular Systems, Eindhoven University of Technology, 5600 MB Eindhoven, The Netherlands; Dutch Institute for Fundamental Energy Research, 5612 AJ Eindhoven, The Netherlands;* orcid.org/0000-0002-1920-5124; Email: r.a.j.janssen@tue.nl

Authors

Pieter J. Leenaers − *Molecular Materials and Nanosystems & Institute for Complex Molecular Systems, Eindhoven University of Technology, 5600 MB Eindhoven, The Netherlands*

Harm van Eersel − *Simbeyond B.V., 5612 AE Eindhoven, The Netherlands*

Junyu Li − *Molecular Materials and Nanosystems & Institute for Complex Molecular Systems, Eindhoven University of Technology, 5600 MB Eindhoven, The Netherlands*

Martijn M. Wienk − *Molecular Materials and Nanosystems & Institute for Complex Molecular Systems, Eindhoven University of Technology, 5600 MB Eindhoven, The Netherlands*

Complete contact information is available at: https://pubs.acs.org/10.1021/acs.macromol.0c01655

Notes

The authors declare no competing financial interest.

■ ACKNOWLEDGMENTS

We thank Gaël Heintges and Dr. Koen Hendriks for valuable discussions and Dr. Mengmeng Li for TEM experiments. The research is partly financed by the NWO Spinoza prize awarded to R.A.J.J. by The Netherlands Organization for Scientific Research (NWO), by the TripleSolar (ERC Advanced Grant 339031) project, and by the Ministry of Education, Culture and Science (Gravity program 024.001.035).

■ REFERENCES

(1) Yan, H.; Chen, Z.; Zheng, Y.; Newman, C.; Quinn, J. R.; Dötz, F.; Kastler, M.; Facchetti, A. A high-mobility electron-transporting polymer for printed transistors. *Nature* **2009**, *457*, 679−686.

(2) Quinn, J. T. E.; Zhu, J.; Li, X.; Wang, J.; Li, Y. Recent progress in the development of n-type organic semiconductors for organic field effect transistors. *J. Mater. Chem. C* **2017**, *5*, 8654−8681.

(3) Ying, L.; Ho, C.-L.; Wu, H.; Cao, Y.; Wong, W.-Y. White polymer light-emitting devices for solid-state lighting: materials, devices, and recent progress. *Adv. Mater.* **2014**, *26*, 2459−2473.

(4) Hu, L.; Wu, Z.; Wang, X.; Ma, Y.; Guo, T.; Ying, L.; Peng, J.; Cao, Y. Deep-blue light-emitting polyfluorenes with asymmetrical naphthylthio-fluorene as chromophores. *J. Polym. Sci., Part A: Polym. Chem.* **2019**, *57*, 171−182.

(5) Li, G.; Zhu, R.; Yang, Y. Polymer solar cells. *Nat. Photonics* **2012**, *6*, 153−161.

(6) Zhao, J.; Li, Y.; Yang, G.; Jiang, K.; Lin, H.; Ade, H.; Ma, W.; Yan, H. Efficient organic solar cells processed from hydrocarbon solvents. *Nat. Energy* **2016**, *1*, 15027.

(7) Havinga, E. E.; ten Hoeve, W.; Wynberg, H. A new class of small band gap organic polymer conductors. *Polym. Bull.* **1992**, *29*, 119−126.

(8) Zhang, Z.-G.; Wang, J. Structures and properties of conjugated donor−acceptor copolymers for solar cell applications. *J. Mater. Chem.* **2012**, *22*, 4178−4187.

(9) Holliday, S.; Donaghey, J. E.; McCulloch, I. Advances in charge carrier mobilities of semiconducting polymers used in organic transistors. *Chem. Mater.* **2014**, *26*, 647−663.

(10) McCulloch, I.; Heeney, M.; Bailey, C.; Genevicius, K.; MacDonald, I.; Shkunov, M.; Sparrowe, D.; Tierney, S.; Wagner, R.; Zhang, W.; Chabinyc, M. L.; Kline, R. J.; McGehee, M. D.; Toney, M. F. Liquid-crystalline semiconducting polymers with high charge-carrier mobility. *Nat. Mater.* **2006**, *5*, 328−333.

(11) Piliego, C.; Holcombe, T. W.; Douglas, J. D.; Woo, C. H.; Beaujuge, P. M.; Fréchet, J. M. J. Synthetic control of structural order in *N*-alkylthieno[3,4-*c*]pyrrole-4,6-dione-based polymers for efficient solar cells. *J. Am. Chem. Soc.* **2010**, *132*, 7595−7597.

(12) Müller, C.; Wang, E.; Andersson, L. M.; Tvingstedt, K.; Zhou, Y.; Andersson, M. R.; Inganäs, O. Influence of molecular weight on the performance of organic solar cells based on a fluorene derivative. *Adv. Funct. Mater.* **2010**, *20*, 2124−2131.

(13) Katsouras, A.; Gasparini, N.; Koulogiannis, C.; Spanos, M.; Ameri, T.; Brabec, C. J.; Chochos, C. L.; Avgeropoulos, A. Systematic analysis of polymer molecular weight influence on the organic photovoltaic performance. *Macromol. Rapid Commun.* **2015**, *36*, 1778−1797.

(14) van Franeker, J. J.; Heintges, G. H. L.; Schaefer, C.; Portale, G.; Li, W.; Wienk, M. M.; van der Schoot, P.; Janssen, R. A. J. Polymer solar cells: solubility controls fiber network formation. *J. Am. Chem. Soc.* **2015**, *137*, 11783−11794.

(15) Jeffries-EL, M.; Sauvé, G.; McCullough, R. D. In-situ end-group functionalization of regioregular poly(3-alkylthiophene) using the

Grignard metathesis polymerization method. *Adv. Mater.* **2004**, *16*, 1017−1019.
(16) Kim, Y.; Cook, S.; Tuladhar, S. M.; Choulis, S. A.; Nelson, J.; Durrant, J. R.; Bradley, D. D. C.; Giles, M.; McCulloch, I.; Ha, C.-S.; Ree, M. A strong regioregularity effect in self-organizing conjugated polymer films and high-efficiency polythiophene:fullerene solar cells. *Nat. Mater.* **2006**, *5*, 197−203.
(17) Ying, L.; Huang, F.; Bazan, G. C. Regioregular narrow-bandgap-conjugated polymers for plastic electronics. *Nat. Commun.* **2017**, *8*, 14047.
(18) Meredig, B.; Salleo, A.; Gee, R. Ordering of poly(3-hexylthiophene) nanocrystallites on the basis of substrate surface energy. *ACS Nano* **2009**, *3* (10), 2881−2886.
(19) Shaheen, S. E.; Brabec, C. J.; Sariciftci, N. S.; Padinger, F.; Fromherz, T.; Hummelen, J. C. 2.5% Efficient organic plastic solar cells. *Appl. Phys. Lett.* **2001**, *78*, 841−843.
(20) An, T. K.; Kang, I.; Yun, H.-J.; Cha, H.; Hwang, J.; Park, S.; Kim, J.; Kim, Y. J.; Chung, D. S.; Kwon, S.-K.; Kim, Y.-H.; Park, C. E. Solvent additive to achieve highly ordered nanostructural semicrystalline DPP copolymers: toward a high charge carrier mobility. *Adv. Mater.* **2013**, *25*, 7003−7009.
(21) Liu, J.; Zhang, R.; Sauvé, G.; Kowalewski, T.; McCullough, R. D. Highly disordered polymer field effect transistors: *N*-alkyl dithieno[3,2-*b*:2′,3′-*d*]pyrrole-based copolymers with surprisingly high charge carrier mobilities. *J. Am. Chem. Soc.* **2008**, *130*, 13167−13176.
(22) Bin, H.; Zhang, Z.-G.; Gao, L.; Chen, S.; Zhong, L.; Xue, L.; Yang, C.; Li, Y. Non-fullerene polymer solar cells based on alkylthio and fluorine substituted 2D-conjugated polymers reach 9.5% efficiency. *J. Am. Chem. Soc.* **2016**, *138*, 4657−4664.
(23) Bulumulla, C.; Gunawardhana, R.; Kularatne, R. N.; Hill, M. E.; McCandless, G. T.; Biewer, M. C.; Stefan, M. C. Thieno[3,2-*b*]pyrrole-benzothiadiazole Banana-shaped small molecules for organic field-effect transistors. *ACS Appl. Mater. Interfaces* **2018**, *10*, 11818−11825.
(24) Sirringhaus, H.; Brown, P. J.; Friend, R. H.; Nielsen, M. M.; Bechgaard, K.; Langeveld-Voss, B. M. W.; Spiering, A. J. H.; Janssen, R. A. J.; Meijer, E. W.; Herwig, P.; de Leeuw, D. M. Two-dimensional charge transport in self-organized, high-mobility conjugated polymers. *Nature* **1999**, *401*, 685−688.
(25) Zhong, H.; Li, C.-Z.; Carpenter, J.; Ade, H.; Jen, A. K.-Y. Influence of regio- and chemoselectivity on the properties of fluoro-substituted thienothiophene and benzodithiophene copolymers. *J. Am. Chem. Soc.* **2015**, *137*, 7616−7619.
(26) Wang, M.; Wang, H.; Yokoyama, T.; Liu, X.; Huang, Y.; Zhang, Y.; Nguyen, T.-Q.; Aramaki, S.; Bazan, G. C. High open circuit voltage in regioregular narrow band gap polymer solar cells. *J. Am. Chem. Soc.* **2014**, *136*, 12576−12579.
(27) Ying, L.; Hsu, B. B. Y.; Zhan, H.; Welch, G. C.; Zalar, P.; Perez, L. A.; Kramer, E. J.; Nguyen, T.-Q.; Heeger, A. J.; Wong, W.-Y.; Bazan, G. C. Regioregular pyridal[2,1,3]thiadiazole π-conjugated copolymers. *J. Am. Chem. Soc.* **2011**, *133*, 18538−18541.
(28) Yuan, J.; Ford, M. J.; Zhang, Y.; Dong, H.; Li, Z.; Li, Y.; Nguyen, T.-Q.; Bazan, G. C.; Ma, W. Toward thermal stable and high photovoltaic efficiency ternary conjugated copolymers: influence of backbone fluorination and regioselectivity. *Chem. Mater.* **2017**, *29*, 1758−1768.
(29) Zhong, H.; Ye, L.; Chen, J.-Y.; Jo, S. B.; Chueh, C.-C.; Carpenter, J. H.; Ade, H.; Jen, A. K.-Y. A regioregular conjugated polymer for high performance thick-film organic solar cells without processing additive. *J. Mater. Chem. A* **2017**, *5*, 10517−10525.
(30) Zhu, D.; Wang, Q.; Wang, Y.; Bao, X.; Qiu, M.; Shahid, B.; Li, Y.; Yang, R. Thiazole-induced quinoid polymers for efficient solar cells: Influence of molecular skeleton, regioselectivity, and regioregularity. *Chem. Mater.* **2018**, *30*, 4639−4645.
(31) Perez, L. A.; Zalar, P.; Ying, L.; Schmidt, K.; Toney, M. F.; Nguyen, T.-Q.; Bazan, G. C.; Kramer, E. J. Effect of backbone regioregularity on the structure and orientation of a donor−acceptor semiconducting copolymer. *Macromolecules* **2014**, *47*, 1403−1410.
(32) Wen, W.; Ying, L.; Hsu, B. B. Y.; Zhang, Y.; Nguyen, T.-Q.; Bazan, G. C. Regioregular pyridyl[2,1,3]thiadiazole-*co*-indacenodithiophene conjugated polymers. *Chem. Commun.* **2013**, *49*, 7192−7194.
(33) Wang, M.; Ford, M.; Phan, H.; Coughlin, J.; Nguyen, T.-Q.; Bazan, G. C. Fluorine substitution influence on benzo[2,1,3]-thiadiazole based polymers for field-effect transistor applications. *Chem. Commun.* **2016**, *52*, 3207−3210.
(34) Qin, T.; Zajaczkowski, W.; Pisula, W.; Baumgarten, M.; Chen, M.; Gao, M.; Wilson, G.; Easton, C. D.; Müllen, K.; Watkins, S. E. Tailored donor−acceptor polymers with an A−D1−A−D2 structure: Controlling Intermolecular interactions to enable enhanced polymer photovoltaic devices. *J. Am. Chem. Soc.* **2014**, *136*, 6049−6055.
(35) Zhou, C.; Zhang, G.; Zhong, C.; Jia, X.; Luo, P.; Xu, R.; Gao, K.; Jiang, X.; Liu, F.; Russell, T. P.; Huang, F.; Cao, Y. Toward high efficiency polymer solar cells: Influence of local chemical environment and morphology. *Adv. Energy Mater.* **2017**, *7*, 1601081.
(36) Lee, J.; Kang, S.-H.; Lee, S. M.; Lee, K. C.; Yang, H.; Cho, Y.; Han, D.; Li, Y.; Lee, B. H.; Yang, C. An ultrahigh mobility in isomorphic fluorobenzo[*c*][1,2,5]thiadiazole-based polymers. *Angew. Chem., Int. Ed.* **2018**, *57*, 13629−13634.
(37) Zhou, C.; Chen, Z.; Zhang, G.; McDowell, C.; Luo, P.; Jia, X.; Ford, M. J.; Wang, M.; Bazan, G. C.; Huang, F.; Cao, Y. Toward high efficiency polymer solar cells: rearranging the backbone units into a readily accessible random tetrapolymer. *Adv. Energy Mater.* **2018**, *8*, 1701668.
(38) Kim, H.; Lee, H.; Seo, D.; Jeong, Y.; Cho, K.; Lee, J.; Lee, Y. Regioregular low bandgap polymer with controlled thieno[3,4-*b*]thiophene orientation for high-efficiency polymer solar cells. *Chem. Mater.* **2015**, *27*, 3102−3107.
(39) Huang, Y.; Zheng, N.; Wang, Z.; Ying, L.; Huang, F.; Cao, Y. Synthesis of regioregular π-conjugated polymers consisting of a lactam moiety via direct heteroarylation polymerization. *Chem. Commun.* **2017**, *53*, 1997−2000.
(40) Ji, Y.; Xiao, C.; Wang, Q.; Zhang, J.; Li, C.; Wu, Y.; Wei, Z.; Zhan, X.; Hu, W.; Wang, Z.; Janssen, R. A. J.; Li, W. Asymmetric diketopyrrolopyrrole conjugated polymers for field-effect transistors and polymer solar cells processed from a nonchlorinated solvent. *Adv. Mater.* **2016**, *28*, 943−950.
(41) Jiang, Z.; Ni, Z.; Wang, H.; Wang, Z.; Zhang, J.; Qiu, G.; Fang, J.; Zhang, Y.; Dong, H.; Lu, K.; Hu, W.; Wei, Z. Versatile asymmetric thiophene/benzothiophene flanked diketopyrrolopyrrole polymers with ambipolar properties for OFETs and OSCs. *Polym. Chem.* **2017**, *8*, 5603−5610.
(42) Ding, S.; Ni, Z.; Hu, M.; Qiu, G.; Li, J.; Ye, J.; Zhang, X.; Liu, F.; Dong, H.; Hu, W. An Asymmetric furan/thieno[3,2-*b*]thiophene diketopyrrolopyrrole building block for annealing-free green-solvent processable organic thin-film transistors. *Macromol. Rapid Commun.* **2018**, *39*, 1800225.
(43) Aoshima, K.; Ide, M.; Saeki, A. Organic photovoltaics of diketopyrrolopyrrole copolymers with unsymmetric and regiorandom configuration of the side units. *RSC Adv.* **2018**, *8*, 30201−30206.
(44) Qiu, G.; Jiang, Z.; Ni, Z.; Wang, H.; Dong, H.; Zhang, J.; Zhang, X.; Shu, Z.; Lu, K.; Zhen, Y.; Wei, Z.; Hu, W. Asymmetric thiophene/pyridine flanked diketopyrrolopyrrole polymers for high performance polymer ambipolar field-effect transistors and solar cells. *J. Mater. Chem. C* **2017**, *5*, 566−572.
(45) Yu, Y.; Wu, Y.; Zhang, A.; Li, C.; Tang, Z.; Ma, W.; Wu, Y.; Li, W. Diketopyrrolopyrrole polymers with thienyl and thiazolyl linkers for application in field-effect transistors and polymer solar cells. *ACS Appl. Mater. Interfaces* **2016**, *8*, 30328−30335.
(46) Yang, F.; Li, C.; Zhang, J.; Feng, G.; Wei, Z.; Li, W. Methylated conjugated polymers based on diketopyrrolopyrrole and dithienothiophene for high performance field-effect transistors. *Org. Electron.* **2016**, *37*, 366−370.
(47) Zhang, A.; Xiao, C.; Wu, Y.; Li, C.; Ji, Y.; Li, L.; Hu, W.; Wang, Z.; Ma, W.; Li, W. Effect of fluorination on molecular orientation of conjugated polymers in high performance field-effect transistors. *Macromolecules* **2016**, *49*, 6431−6438.

https://dx.doi.org/10.1021/acs.macromol.0c01655
Macromolecules 2020, 53, 7749−7758

(48) Feng, G.; Xu, Y.; Wu, Y.; Li, C.; Yang, F.; Yu, Y.; Ma, W.; Li, W. Enhancing the photovoltaic performance of binary acceptor-based conjugated polymers incorporating methyl units. *RSC Adv.* **2016**, *6*, 98071−98079.
(49) Aoshima, K.; Nomura, M.; Saeki, A. Regioregularity and electron deficiency control of unsymmetric diketopyrrolopyrrole copolymers for organic photovoltaics. *ACS Omega.* **2019**, *4*, 15645−15652.
(50) Hayoz, P.; Aebischer, O. F.; Düggeli, M.; Turbiez, M. G. R.; Fonrodona Turon, M.; Chebotareva, N. Pyrrolopyrrole derivatives, their manufacture and use as semiconductors. PCT Int. Appl., WO 2010115767 A1, 14 Oct 2010.
(51) Hendriks, K. H.; Li, W.; Heintges, G. H. L.; van Pruissen, G. W. P.; Wienk, M. M.; Janssen, R. A. J. Homocoupling defects in diketopyrrolopyrrole-based copolymers and their effect on photovoltaic performance. *J. Am. Chem. Soc.* **2014**, *136*, 11128−11133.
(52) Hendriks, K. H.; Heintges, G. H. L.; Gevaerts, V. S.; Wienk, M. M.; Janssen, R. A. J. High-molecular-weight regular alternating diketopyrrolopyrrole-based terpolymers for efficient organic solar cells. *Angew. Chem., Int. Ed.* **2013**, *52*, 8341−8344.
(53) Hendriks, K. H.; Wijpkema, A. S. G.; van Franeker, J. J.; Wienk, M. M.; Janssen, R. A. J. Dichotomous role of exciting the donor or the acceptor on charge generation in organic solar cells. *J. Am. Chem. Soc.* **2016**, *138*, 10026−10031.
(54) Willems, R. E. M.; Weijtens, C. H. L.; de Vries, X.; Coehoorn, R.; Janssen, R. A. J. Relating frontier orbital energies from voltammetry and photoelectron spectroscopy to the open-circuit voltage of organic solar cells. *Adv. Energy Mater.* **2019**, *9*, 1803677.
(55) Saes, B. H. W.; Wienk, M. M.; Janssen, R. A. J. The effect of α-branched side chains on the structural and opto-electronic properties of poly(diketopyrrolopyrrole-*alt*-terthiophene). *Chem. - Eur. J.* **2020**, DOI: 10.1002/chem.202001722.
(56) Li, W.; Hendriks, K. H.; Furlan, A.; Wienk, M. M.; Janssen, R. A. J. High quantum efficiencies in polymer solar cells at energy losses below 0.6 eV. *J. Am. Chem. Soc.* **2015**, *137*, 2231−2234.
(57) Li, W.; Hendriks, K. H.; Wienk, M. M.; Janssen, R. A. J. Diketopyrrolopyrrole polymers for organic solar cells. *Acc. Chem. Res.* **2016**, *49*, 78−85.
(58) Murgatroyd, P. N. Theory of space-charge-limited current enhanced by Frenkel effect. *J. Phys. D: Appl. Phys.* **1970**, *3*, 151−156.
(59) Blakesley, J. C.; Castro, F. A.; Kylberg, W.; Dibb, G. F. A.; Arantes, C.; Valaski, R.; Cremona, M.; Kim, J. S.; Kim, J.-S. Towards reliable charge-mobility benchmark measurements for organic semiconductors. *Org. Electron.* **2014**, *15*, 1263−1272.

https://dx.doi.org/10.1021/acs.macromol.0c01655
Macromolecules 2020, 53, 7749−7758